Comparison of continuous and discrete modeling strategies for the structural assessment of a masonry vault under dynamic seismic loading

Angela Ferrante, Frédéric Dubois, Pierre Morenon

RESEARCH ARTICLE

Comparison of continuous and discrete modeling strategies for the structural assessment of a masonry vault under dynamic seismic loading

Angela Ferrante[a], Frédéric Dubois[a] and Pierre Morenon[b,c]

[a] LMGC, CNRS, Univ. Montpellier, Montpellier, France; [b] Université de Toulouse, UPS, INSA, LMDC, 135, avenue de Rangueil, F-31 077 Toulouse Cedex 04, France; [c] Toulouse Tech Transfer, 118 route de Narbonne, CS 24246, 31432 Toulouse Cedex 04, France

ARTICLE HISTORY
Compiled July 17, 2024

ABSTRACT
To begin, the paper introduces methodologies employing both homogeneous continuous Finite Element Method (FEM) and block-by-block Discrete Element Method (DEM) to model masonry behaviors. In the continuous approach, the masonry is modeled as an anisotropic damageable material (homogeneous or not). In contrast, the block-based approach represents rigid blocks interacting through contact joints governed by frictional cohesive behaviors. The DEM framework allows for significant displacements, rotations, and complete detachments of blocks, aspects often overlooked in traditional FEM models. The primary application of this research involves the seismic assessment of a masonry cross vault. Notably, the numerical results exhibit the approach's capability to provide realistic predictions of failure mechanisms, crucial for retrofitting efforts. This includes an accurate representation of the actual cracking pattern, accounting for significant displacements. The numerical implementation is accessible through the open-source LMGC90 software. Comparative analyses are then carried out, focusing on the strengths and weaknesses of FEM macro-modeling (continuous homogeneous description) and DEM utilizing rigid blocks.

KEYWORDS
Discrete Element Method; Finite Element Method; Damage model; Non-Smooth Contact Dynamics; LMGC90; Masonry

1. Introduction

Examining the dynamic nonlinear behavior of structures, particularly masonry vaults, is a multifaceted undertaking. An imperative aspect of this pursuit lies in advancing our comprehension of these structures, as it holds significance for preserving cultural heritage, appraising the seismic resilience of existing civil engineering structures within high-risk European regions, and scrutinizing the seismic performance of novel structures. Masonry vaults, intrinsic to historical edifices, have been evaluated through diverse methodologies and experimental assessments documented in existing literature (D'Ayala and Tomasoni (2011); Gaetani et al. (2016); Rossi et al. (2016)). This study

CONTACT Angela Ferrante. Email: angela.ferrante.eng@gmail.com

digs into the application of both Finite and Discrete Element Methods (FEM and DEM) within our simulation tool, integrated into the open-source LMGC90 software (Dubois et al. (2018)). The Finite Element Method, as conventionally employed, adopts a Continuous Homogeneous Model (CHM). In this paradigm, masonry is treated as a homogenized material (Sellier et al. (2013, 2022)), and the model captures a nonlinear response by intertwining plasticity and orthotropic damages, separating behaviors under tension and shear/compression. Conversely, the Discrete Element Method operates on a Block-Based Model (BBM), offering a discrete block-by-block representation of masonry. It meticulously considers mechanical interactions between blocks, accounting for failure and cracking patterns occurring at the block-mortar interface (Ferrante et al. (2021a,b)).
The main application of this work focuses on the modeling and the results of the SERA (Seismology and Earthquake Engineering Research Infrastructure Alliance for Europe) blind test (Bianchini et al. (2023a); Bianchini et al. (2023b)) using CHM and BBM approaches. The blind test specifically focuses on the seismic assessment of a masonry cross vault, allowing for an in-depth exploration of the advantages and disadvantages inherent in various modeling approaches. This evaluation extends beyond several model comparisons, including nuanced considerations of micro- and macro-modeling paradigms, such as the block-based model or continuous homogeneous model. Reviews of existing numerical approaches are proposed in several papers (for example Roca et al. (2010); D'Altri et al. (2019))

2. Existing models

In this section, we recall the main ingredients of the continuous and block based models we used to simulate the nonlinear behavior of the masonry.

2.1. *FEM - Damage and plasticity model (Endo3D)*

The phenomenological behavior of the material, whether it be masonry, block, or joint, is achieved through a damageable elasto-plastic phenomenological model developed by Sellier (Sellier et al. (2022)), adapted from Sellier's previous work (Sellier et al. (2013)). In this model, the elasto-plastic behavior is constrained to positive or null hardening and is articulated in terms of effective stresses. Notably, damage emerges as a consequence of plastic strain—a difference from the conventional approach where damage is often attributed to elastic strain. The stress-strain softening, in this context, is solely a result of damages, including crack opening, crack re-closure, and settlement, all of which impact effective stresses (see Equation 1). The model dissociates the intricate behavior of the material through the following mechanisms:

(1) Tensile Cracking : Governed by three Rankine criteria in principal positive stresses, leading to plastic strains and localized openings of cracking. Damages $\boldsymbol{D}^t$ manifest during the softening phase subsequent to reaching tensile strength.
(2) Crack re-closure Cracking: Controlled by three Rankine criteria in principal negative stresses. Enables the recovery of rigidity in compression after the re-closure of a tensile crack. Damages $\boldsymbol{D}^r$ are associated with this phase.
(3) Shear-Compression Cracking: Driven by the Drucker-Prager criterion, employing non-associated plastic flow (Drucker and Prager (1952)). The plastic strains

calculated lead to an isotropic induced damage D^{sc}.

$$\sigma_{ij} = (1 - D^{t}_{prepeak}).(\mathbf{1} - \boldsymbol{D}^{t})_{ijkl}.\sigma^{+}_{kl} + (1 - D^{sc}_{prepeak}).(1 - D^{sc}).(\mathbf{1} - \boldsymbol{D}^{r})_{ijkl}.\sigma^{-}_{kl} \quad (1)$$

This phenomenological model offers a comprehensive understanding of the material's response to various loading conditions, encompassing tension, compression, and shear. It establishes an approach where damage is intricately linked to plastic strain, providing a more realistic representation of the material's behavior under different stress states. The utilization of multiple criteria for tensile and compressive behaviors demonstrates the model's ability to capture the complexity of existing material response, contributing to a nuanced and accurate representation in structural simulations.

The undamaged material under consideration is treated as isotropic; however, when subjected to a load, it induces an orthotropic damage that can rotate along the load path. This model accounts for the asymmetry in tensile/compressive behavior, providing a comprehensive representation of the material response (Equation 1). To further enhance realism, pre-peak damages ($D^{t}_{prepeak}$ and $D^{sc}_{prepeak}$) and plastic strains are incorporated, allowing the simulation to mimic the actual state of materials under tension or compression. Consequently, the total stress is influenced by distinct damage variables that are carefully managed within the framework of this model. A feature of this model is its flexibility in setting the ratio between plasticity and pre-peak damage in compression, offering a nuanced control mechanism to reproduce the behavior of the material under different loading conditions. Moreover, the model incorporates energy regularization in tension using the Hillerborg method (Hillerborg et al. (1976)). This regularization method leverages the size of the finite element in the principal tensile direction. By multiplying this size and the plastic strain, the model determines crack opening.
Figure 1 provides a visual representation of the model's response under cyclic uniaxial loading, illustrating its evolving behavior.

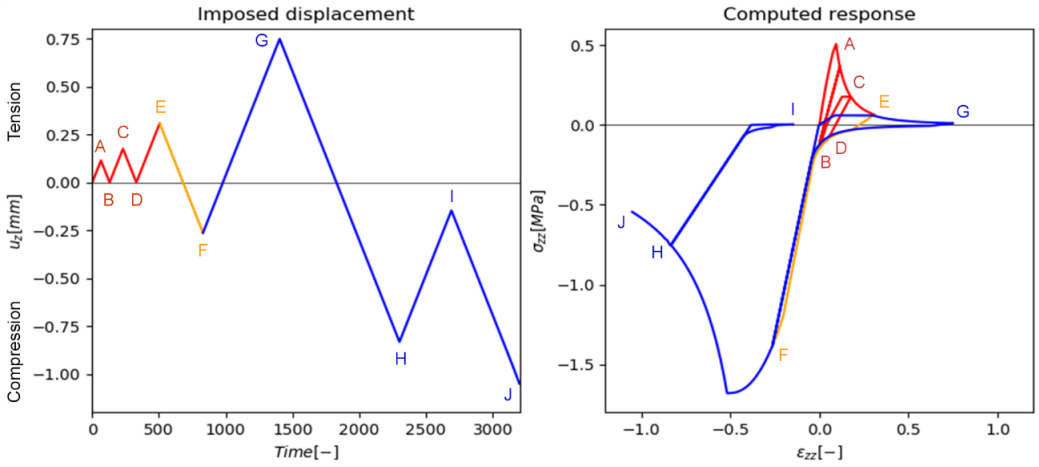

Figure 1. Response of the endo3D model for a uniaxial cyclic test

This model, designed for macro simulation, has been previously utilized for quasi-static calculations in the analysis of vaulted structures such as bridges (Domede et al. (2013)) and churches (Parent et al. (2023)) Its first application with dynamic loading scenarios, showcase its adaptability and robustness in capturing the intricate dynamics of structures under varying loading conditions. This application with dynamic loading

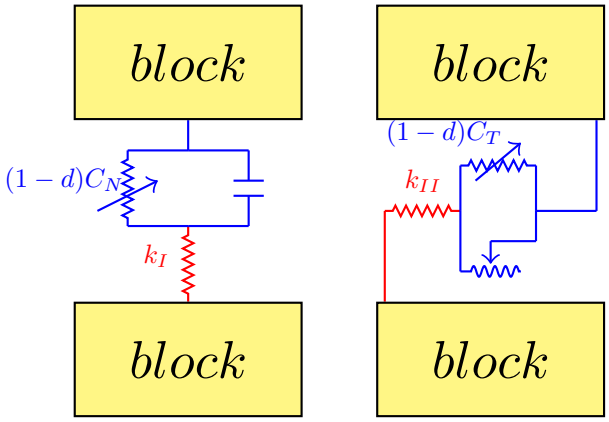

Figure 2. Normal (left) and tangential (right) behaviour of the FCZM

extends the utility of the model, contributing to a more comprehensive understanding of its capabilities in diverse structural analyses, allowing for example the modal analysis of the damaged structure after an earthquake.

The main mechanical properties needed for the model are summarized in Table 1.

2.2. *DEM - Frictional Cohesive Zone model*

The numerical model presented here is complex, employing a block-by-block discretization strategy for masonry, coupled with an interaction model that meticulously characterizes the contact between blocks, simulating the frictional and cohesive dynamics of the mortar-block interface. Traditionally, blocks are treated as rigid entities, although there is flexibility in considering them as deformable, modeled by finite elements. The mortar joints and block/mortar interfaces are amalgamated into a contact interaction, called the Frictional Cohesive Zone Model (FCZM). The behavior of the brick-mortar interface is detailed, encapsulating frictional contact and damage response in tandem with a decreasing exponential evolution, a consequence of the progressive damage inherent in quasi-brittle materials (Venzal et al. (2020)). To further enhance the model's fidelity, a linear spring is introduced to replicate the behavior of mortar joints under both compression and traction. The interaction model delineating the behavior between blocks is characterized by a linear, damageable, and post-rupture frictional pattern specific to masonry joints. This model draws inspiration from a recent extension of Venzal's work and is structured around a linear deformable spring configured in series with a contact cohesive joint (Boukham et al. (2023)), as depicted in Figure 2. This comprehensive approach captures the intricacies of blocs interactions, providing a foundation for a realistic representation of structural responses.

In this conceptual framework, the cohesive strength undergoes a progressive reduction, following an elastic response, contingent upon the evolution of a damage variable denoted as d. This variable serves as an indicator of the mechanical degradation of the interface, representing the advancement of cracks within the material. The formulation of the hard contact joint adopts a modified frictional contact model. In this representation, $\boldsymbol{\sigma}$ represents the contact force vector, σ_N^{coh} and $\boldsymbol{\sigma}_T^{coh}$ respectively denote the normal and tangential cohesive strengths, $[\boldsymbol{u}]$ signifies the displacement jump

at the interface, d characterizes the damage parameter, μ_c represents the frictional coefficient, and n serves as a parameter encapsulating the coupling between cohesive and frictional behaviors. The constitutive equations governing this model are detailed below.

- Equation 2 describes the normal part of the cohesive interaction law while Equation 3 describes the tangential part of the cohesive interaction law.

$$\sigma_N + \sigma_N^{coh} \geq 0 \perp 0 \leq [u_N] \tag{2}$$

$$\begin{aligned} \|\boldsymbol{\sigma}_T + \boldsymbol{\sigma}_T^{coh}\| &\leq \mu(d)(\sigma_N + \sigma_N^{coh}) \\ \text{if } \|\boldsymbol{\sigma}_T + \boldsymbol{\sigma}_T^{coh}\| < \mu(d)(\sigma_N + \sigma_N^{coh}) &\text{ then } \boldsymbol{\mathcal{V}_t} = 0 \\ \text{else } \exists \lambda \geqslant 0, \boldsymbol{\mathcal{V}_t} &= -\lambda(\boldsymbol{\sigma}_T + \boldsymbol{\sigma}_T^{coh}) \end{aligned} \tag{3}$$

- Equation 4 gives the evolution of the friction coefficient with respect to the damage.

$$\mu(d) = d^n \mu_c \tag{4}$$

- Equation 5 gives the evolution of the cohesive strengths within the admissible domain, with respect to the displacement jumps and for a given damage.

$$\sigma_N^{coh} = (1-d) C_N [u_N] \; and \; \boldsymbol{\sigma}_T^{coh} = (1-d) \boldsymbol{C}_T [\boldsymbol{u}_T] \tag{5}$$

- Once the cohesive strength reaches the limit of the admissible domain the damage evolve. Equation 6 is a generic damage evolution function (in out work a decreasing exponential).

$$d = g([\mathbf{u}]; \mathbf{d}) \tag{6}$$

In instances of combined traction and shear loading, the interface response manifests as a blend of mode I (normal component) and mode II (shear component). The parameters governing this mixed-mode model are derived through a meticulous computation involving a mixing ratio, in conjunction with two key criteria: a damage initiation criterion and a failure criterion. These criteria play a crucial role in estimating the failure energy in mixed mode, thereby contributing to a comprehensive characterization of the interface response under complex loading conditions. Moreover, when subjected to combined compression and shear loading, the stress-displacement relationship of the interface takes into account the intricate interplay between the cohesive behavior of mode II and the frictional behavior (Coulomb's friction). This consideration is made relative to the damage level sustained by the interface. The integration of these behaviors provides a holistic understanding of the structural response, acknowledging the coupling effects between cohesive and frictional mechanisms, and contributing to a nuanced representation of the material's behavior under varied loading scenarios.

In the present study we consider rigid blocks and, following Lourenço (Lourenço and Rots (1997)), we compute k_I and k_{II} to recover the overall stiffness:

$$k_I = \frac{E_u E_m}{t_m(E_u - E_m)} \; k_{II} = \frac{G_u G_m}{t_m(G_u - G_m)} \tag{7}$$

where E_u and E_m (resp. G_u and G_m) are Young's moduli (resp. shear moduli) of the unit and mortar, and t_m is the thickness of the mortar.

The entire system, comprising all blocks interconnected through these interactions, is systematically solved using the Non-Smooth Contact Dynamics method (NSCD) algorithm, constituting the foundational framework of the LMGC90 software (Dubois and Jean (2006)). This method employs an implicit time integrator and the Non-Linear Gauss Seidel contact solver. The NSCD algorithm (Jean (1999); Moreau (1988); Dubois et al. (2018)) turns out to be decisive in managing non-regularized frictional contacts within the system, offering a robust and versatile solution for dynamic simulations.

3. Cross vault seismic assessment

3.1. *Experimental setup and numerical model*

The geometry of the cross vault is recreated in a 3D model, referencing the drawings and specifications provided in the mock-up available on the blind prediction website (Sera project (2021); Bianchini et al. (2023a); Bianchini et al. (2023b)) (refer to Fig.3). The representation of the numerical discrete and continuous models is depicted in Fig.3 c) and d), respectively. In the discrete model, the stereotomy involves an arrangement of discrete extended blocks and zero-thickness joints managed by punctual contacts, as detailed in Fig. 3 c). This arrangement, known as orthogonal weaving, directly transmits thrusts to the supports, concentrating loads into the four corners of the vault. The extended blocks consider the brick units and the mortar thickness, with dimensions of $0.55\times0.12\times0.24$ m^3. This sizing maintains the geometry identical to the real structure. Subsequently, a comparable 3D model is constructed as a continuum of solid finite elements. The infill, supports, masses, and piers are represented using simplified geometries of equivalent global shapes, disregarding intricate details such as the arrangement of bricks for the masonry parts (see Fig.3 b)). Steel profiles, frames, connectors, and wheels are not explicitly modeled using 3D elements. Instead, these elements are incorporated into the numerical model through equivalent relations and boundary conditions, ensuring that their behaviors are simulated accurately. An exception is made for the discrete model, where steel bars are modeled using 3D equivalent interactions, as illustrated in Fig.3 c). This approach ensures a realistic representation of the steel bars within the discrete model.

The discrete model of the mock-up comprises a total of 1242 blocks and 14532 punctual contacts. In plan, its dimensions measure 3.55 x 4.04 m^2. The masonry cross vault specifically consists of 1230 blocks, with the vault's plan dimensions being approximately 3.5 x 3.5 m^2, and a constant thickness of 0.12 m. The remaining 12 blocks serve various purposes: four for filling, four for supports, two for piers, and two for masses.

For the finite element model, tetrahedral meshes with an average size of 0.05 m are employed. The detailed numerical model encompasses 35454 nodes and 143390 degrees of freedom. The boundary conditions are configured to replicate the experimental setup, with masses allowed to slide freely in two directions on the xy plane using wheels. The piers are firmly connected to the shaking table, thus fixed in the z-direction for masses and x- and z-directions for piers. The supports are perfectly connected to the piers, masses, and filling. Steel bars play a crucial role in linking masses to one another and to the piers, preventing rotations of the supports.

The discrete model of the masonry vault may be utilized for analyses conducted in

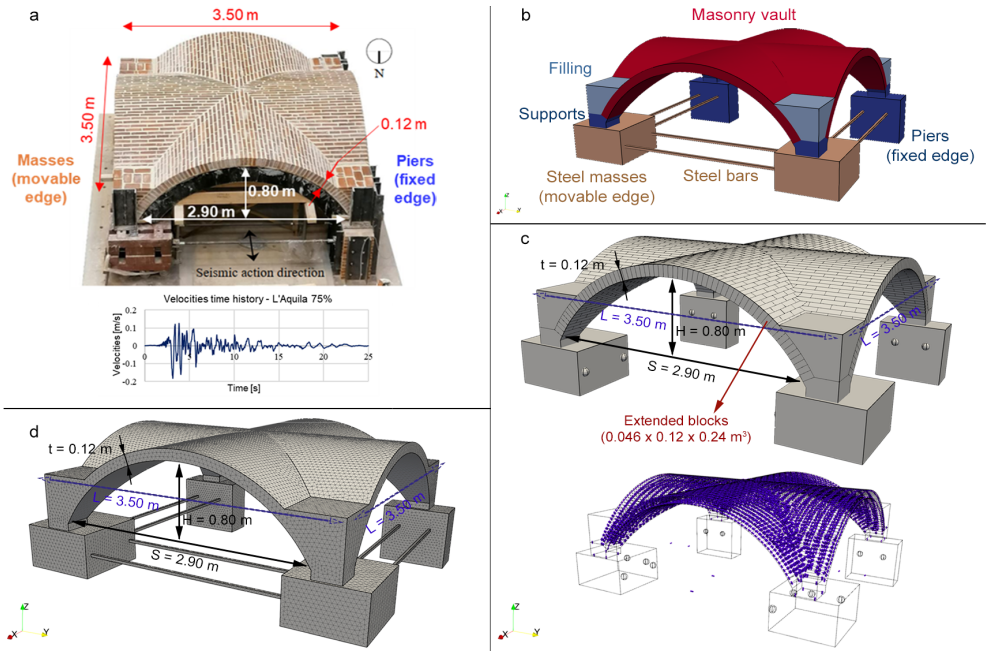

Figure 3. a) Geometry of the experimental groin vault and plot of the uniaxial velocity evolution with respect to time. Detailed drawings of b) mock-up materials as adopted in both numerical modeling techniques, c) the discrete model and its contacts, d) the continuum geometry.

both the classical DEM framework, employing rigid blocks, and the hybrid approach with deformable blocks. In both strategies, the contacts are governed by FCZM. Similarly, the macro-model of the vault is defined by the masonry material parameters of the endo3D model. Other components of the mock-up are modeled as perfectly rigid and elastic in the discrete and continuum approaches, respectively.

The 3D meshes are generated using the open-source GMSH tool, and both modeling strategies are implemented using the open-source LMGC90 code. This integrated approach ensures a comprehensive and accurate representation of the structural response under different loading conditions.

The seismic input, corresponds to the one applied on the shaking table test conducted on the full-scale masonry cross vault (Sera project (2021); Bianchini et al. (2023a)). It is applied at the piers of the models in the y-direction. The dynamic action extends over a total duration of 25 seconds, and the Peak Ground Velocity (PGV) is set at -0.182 m/s, representing 75% of the amplitude-scaled record from the L'Aquila earthquake occurred on April 6, 2009.

3.2. *Calibration process*

To calibrate and validate the proposed phenomenological approach, various real behaviors observed in experimental tests have been replicated. These include compression and traction tests conducted on both bricks and joints, axial compression tests on walls, confined shear tests on triplets, and diagonal compression tests on walls (Bianchini et al. (2023a)). The experimental investigations are focused on the masonry material and its constituent components, such as clay bricks and mortar. These tests adhere to international standards to ensure robust and standardized procedures. For the hardened mortar, a three-point bending test and a compression test were con-

ducted. The prismatic brick and masonry triplet underwent compression and triplet tests, respectively. The parameters derived from these experimental procedures are indispensable for defining the damage model's behavior for both mortar and bricks. Furthermore, homogenized parameters for a masonry wallet are deduced from axial compression and diagonal compression tests. These comprehensive tests and their corresponding parameters serve as the foundation for the calibration and validation of the phenomenological approach. By replicating this set of real-world behaviors, the proposed model aims to capture the intricacies and complexities of masonry structures, providing a robust and reliable simulation tool for various loading conditions.

Thus, in summary, the numerical replication of the experimental direct tensile test, carried out on two blocks joined by a mortar joint, allows the FCZM Mode I cohesive parameters to be estimated. And, a shear test performed on a triplet of blocks assembled by two mortar joints, allows the Mode II cohesive and frictional parameters to be estimated. In the same way, the numerical calibration of some parameters, such as the tensile fracture energy and the re-closure crack energy, are deduced by sensitivity analyses performed starting from the experimental tests available in the blind prediction competition. And, based on more experimental data, a key point for future works is to discuss in more detail the calibration process for these advanced models and the correlations between their parameters.

The values of the parameters used are presented in Table 1 and Table 2.

Table 1. Main mechanical properties of the homogenized material (CHM model) Sellier et al. (2013).

Mechanical properties	Notation	Value	Unit
Bulk Density	ρ	2255	$kg.m^{-3}$
Homogenized Young modulus	E	2.667	GPa
Poisson coefficient	ν	0.2	–
Compressive strength	R_c	9.1	MPa
Compressive peak strain	ϵ_c^{peak}	0.8e-2	–
Druker-Prager confinement coefficient	δ	0.9	MPa
Dilatancy for non associated Drucker-Prager plastic flow	β	0.2	MPa
Tensile strength	R_t	0.31	MPa
Tensile Fracture energy	G_{f_t}	4.5	$J.m^{-2}$
Tensile peak strain	ϵ_t^{peak}	1.16e-4	–
Stress to reclose a crack	R_r	0.3	MPa
Energy to reclose a crack	G_{f_r}	3.6	$J.m^{-2}$

Table 2. Main mechanical properties of block/mortar interface (BBM model).

Mechanical properties	Notation	Value	Unit
Mode I (tension) maximum strength	σ_I	0.12	MPa
Mode I (tension) cohesive energy	G_I	2.0	$J.m^{-2}$
Mode II (shear) maximum strength	σ_{II}	0.28	MPa
Mode II (shear) cohesive energy	G_{II}	40.0	$J.m^{-2}$
Friction coefficient	μ_c	0.785	–

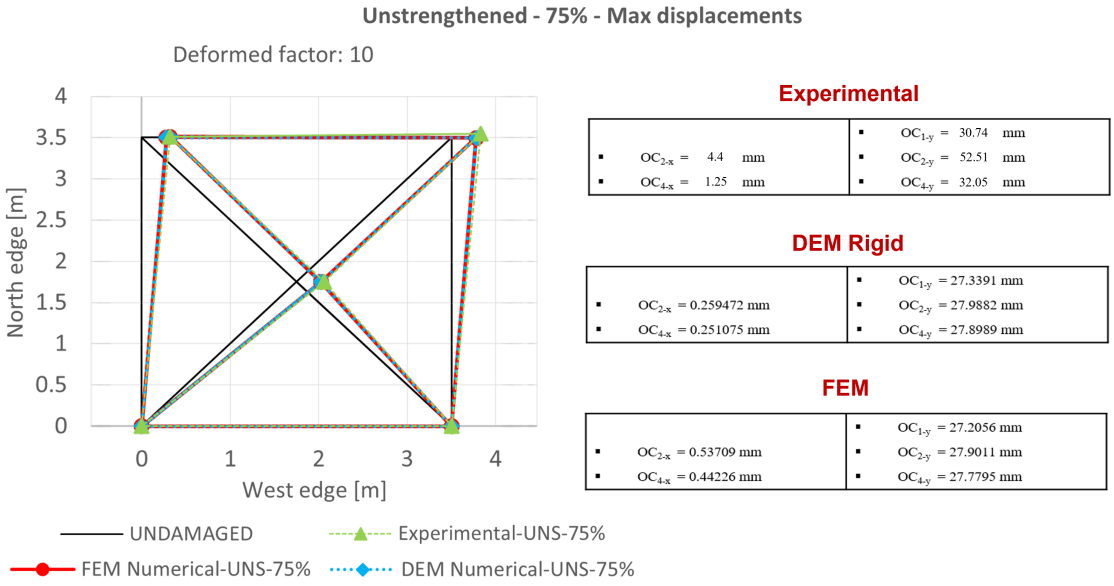

Figure 4. Comparison of the cross vault experimental and numerical displacements monitored during the nonlinear dynamic input applied.

3.3. *Results*

Here are given the results of the two distinct models implemented for the meso and macro modeling approaches. For the meso modeling, involving rigid blocks (BBM), the FCZM for the interfaces is employed. Conversely, for the macro modeling, the homogenized endo3D model (CHM) is applied. This approach provides a comprehensive overview of the proposed models, and the results are analyzed in this section.

3.3.1. Displacements and accelerations

The comparison of the monitored displacements shown in the Fig. 4 confirms that the dynamic responses of the structure simulated by FEM and DEM approaches are close to the experimental real dynamic response. The main displacements are observed in the Y direction. The comparison between the experimental and the model accelerations at two points (center and corner of the vault) in this direction (Fig. 5, shows a good amplitude of the PGA. The amplitude of the DEM's acceleration is a little too strong in the first seconds but rather faithful at the end of the earthquake. Conversely, the FEM model seems to reproduce the good behavior regarding the acceleration of the first seconds and in particular the peak of acceleration, the accelerations of the second part of the test seem slightly overestimated.

3.3.2. Cracking

A concise comparison of the numerical damages between the meso- and macro-models at the end of the dynamic action is presented in Fig. 7 and Fig. 4. The results, in Fig. 7, highlight a commendable match in the failure mechanisms, quite faithful in the matching crack positions for the vault in both models. The adopted approaches effectively reproduce mainly the shear failure of the vault, as illustrated in Fig. 6, emphasizing a pronounced presence of damage along the diagonal sections of the vault.

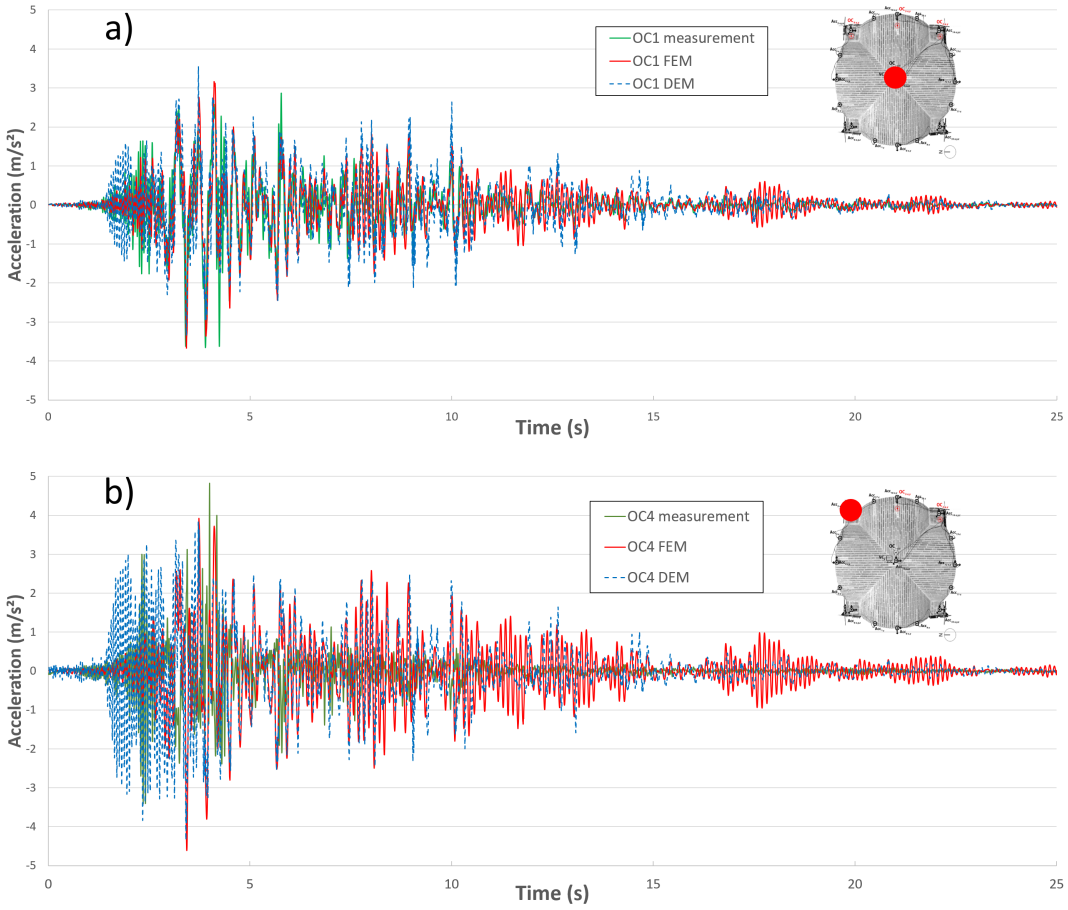

Figure 5. Comparison of the experimental and numerical accelerations monitored during the nonlinear dynamic input applied at a) OC1 (center of the vault) b) OC4 (one of the vault corner).

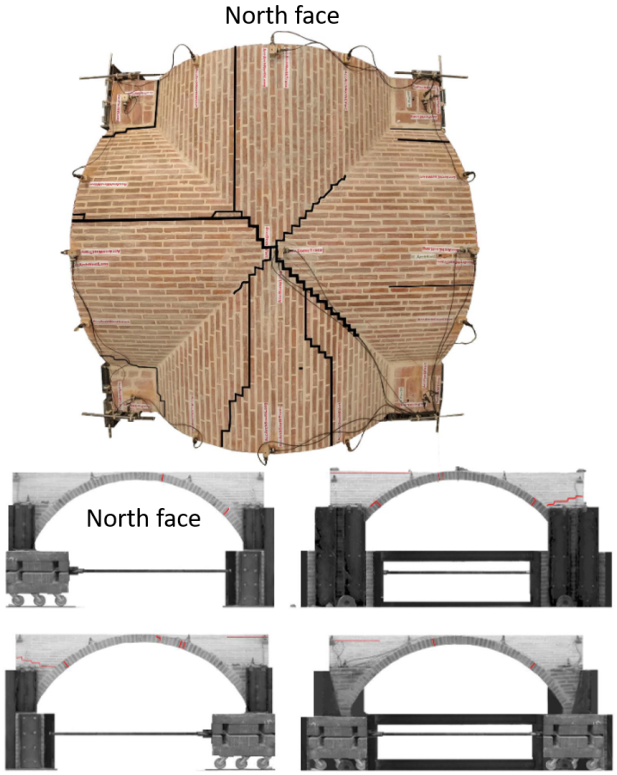

Figure 6. Experimental cracking of the cross vault at the end of the seismic input applied (75% of L'Aquila one) Bianchini et al. (2023b).

This consistency in failure patterns between the meso- and macro-models underscores the reliability and effectiveness of both modeling strategies in capturing and predicting the seismic response and damage evolution of the masonry cross vault.

The detailed views depicted in Fig. 7, Fig. 8 and Fig. 9 provide insights into the numerical hinges of the cross vault in both the meso- and macro-models. As in Fig. 8, the meso-model facilitates a more straightforward examination of the activated hinges and their temporal evolution, crucial for understanding the collapse mechanism of the structure. Notably, the macro-model approximately replicates the location of the hinges observed in the meso-model. This alignment suggests that the macro-model captures the critical features of the hinge locations, contributing to a consistent representation of the structural response and collapse mechanism.

Additionally, the re-closure of the cracking openings for the macro approach, managed by the endo3D model, is illustrated in Fig. 9. At 3.4 seconds into the seismic input application (Fig. 9), the diagonal cracks undergo re-closure. Subsequently, the cracks reach their maximum opening at 3.7 seconds (Fig. 9), and by 3.8 seconds (Fig. 9c), the cracks re-close and then reopen in the opposite diagonal section.

The behaviors depicted in Fig. 9 correspond to the Peak Ground Velocity (PGV) in positive and then negative directions. These dynamic representations provide valuable insights into the evolution of cracking patterns and re-closure mechanisms, contributing to a comprehensive understanding of the structural response under seismic loading conditions.

In the end, both methods are capable of a realistic predicting failure mechanisms and displacement capacity of masonry structures.

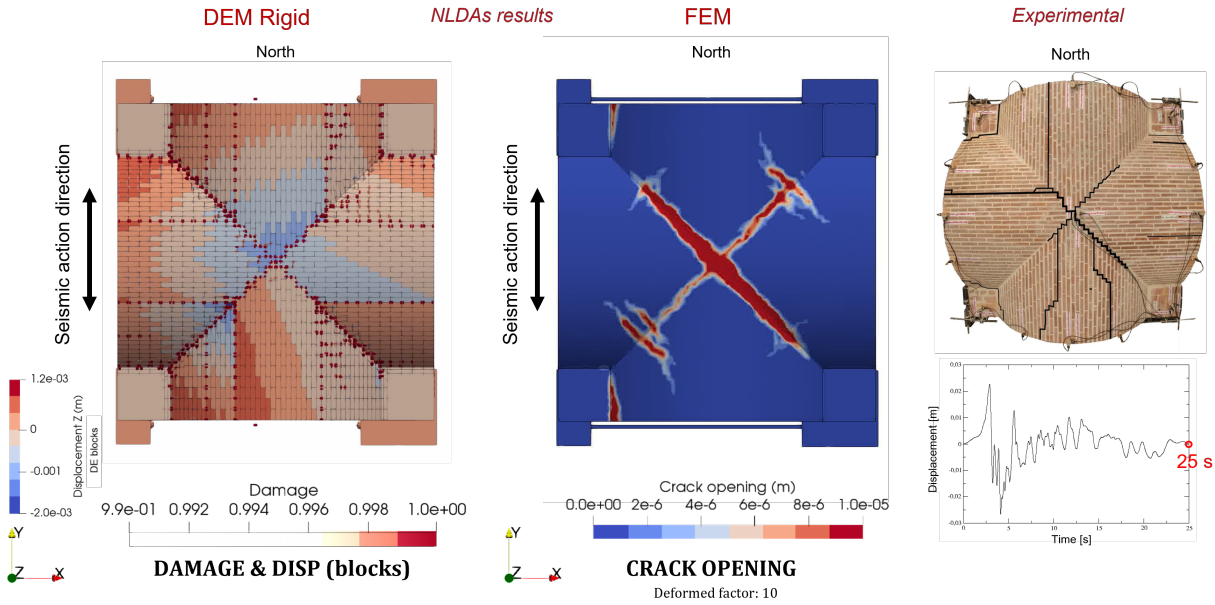

Figure 7. Comparison of the cross vault numerical damages of the meso- and macro-model at the end of the seismic input applied in the nonlinear dynamic analyses performed (top view).

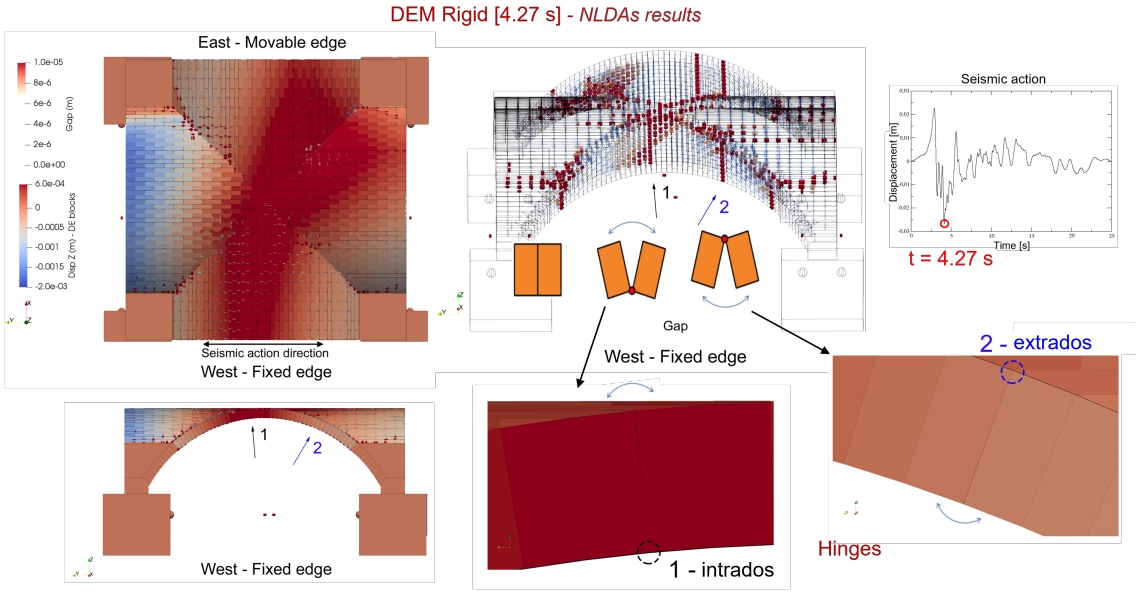

Figure 8. Location of the activated hinges (opening and re-closing) for the DEM model at the 4.27 s of the seismic input applied in the nonlinear dynamic analyses performed (top and lateral views).

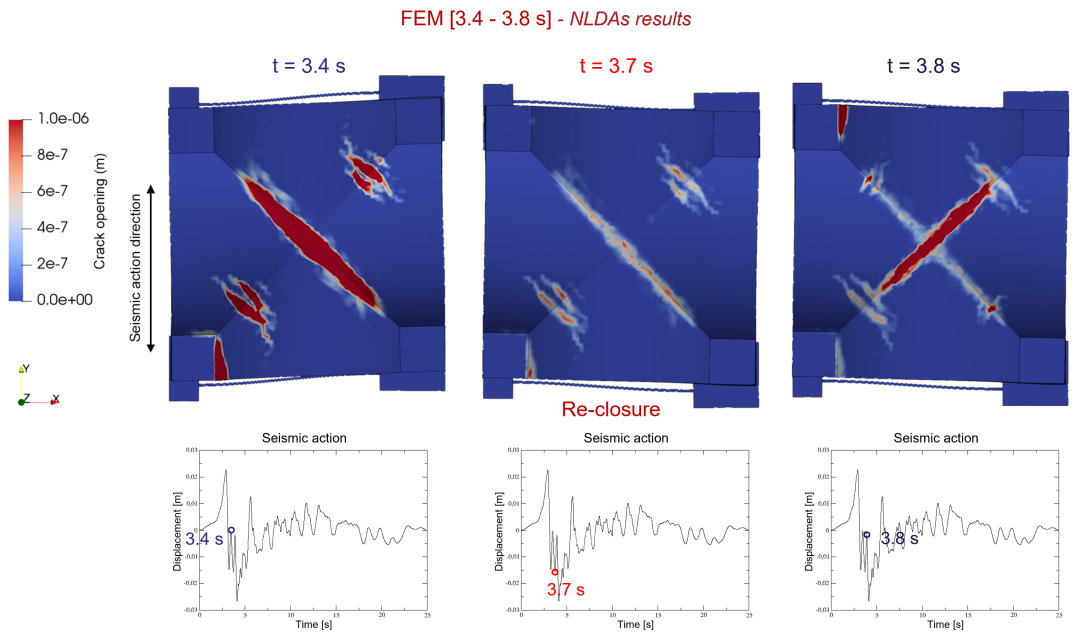

Figure 9. Re-closure of the cracking opening for the FEM model at 3.4 s, 3.7 s and 3.8 s of the seismic input applied in the nonlinear dynamic analyses performed (top view).

3.3.3. Modal analysis

The modal analysis is computed with the FEM model thanks to the simplicity to obtain eigenfrequencies and modes. For the DEM model, this analysis needs harmonic calculations using a frozen damaged. This method is more time consuming and is not implemented automatically in the DEM code for now. The first eigenfrequency (first global mode is shear, Fig. 10) calculated for the sound structure with the macro-model is 6.08 Hz compared to 6.15 Hz for the experimental measurement. The Young's modulus of the masonry was fitted to the static test, so the calibration appears to be correct. Once the vault has been damaged by the 75% of L'Aquila earthquake, the numerical value decreases to 5.35 Hz (an isotropic damage using the maximum damage of each Gauss point is used only for this modal analysis Fig. 11) and the experimental value reaches 5.57 Hz. The damage to the vault reduces the first eigenfrequency of respectively 9.43% for the real vault and 12.00% using the macro-model. The main effects of cracking on the modal analysis seem to be fairly well reproduced in the calculation at the structural scale.

4. Conclusion

The work presented in this paper concerns the modeling of a blind test on the dynamic behavior of a masonry vault using either a continuous homogenized finite elements model or a block based discrete elements model. It highlights the faithfulness of the results obtained in terms of displacements, cracking and modal analysis. Promising results have been obtained for the groin vault using the cohesive zone model in DEM and the endo3D model in FEM simulations. Both advanced models have demonstrated their efficiency in the seismic assessment of vaults and accurately reproducing failure mechanisms in these structural elements.

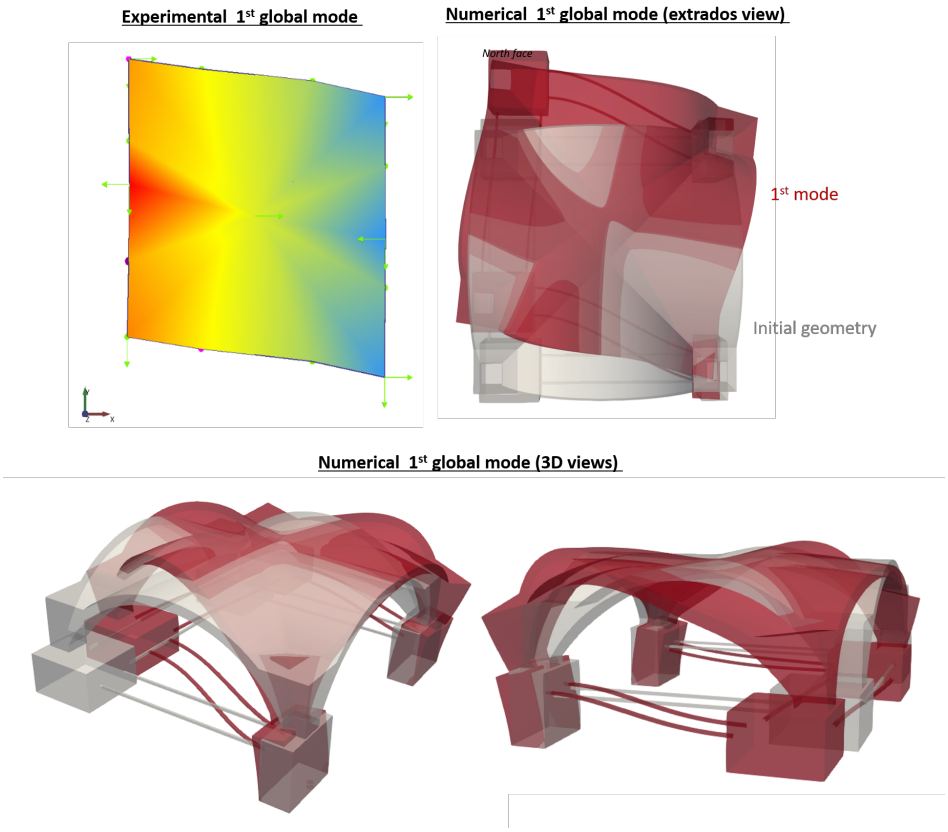

Figure 10. First mode shape (shear)

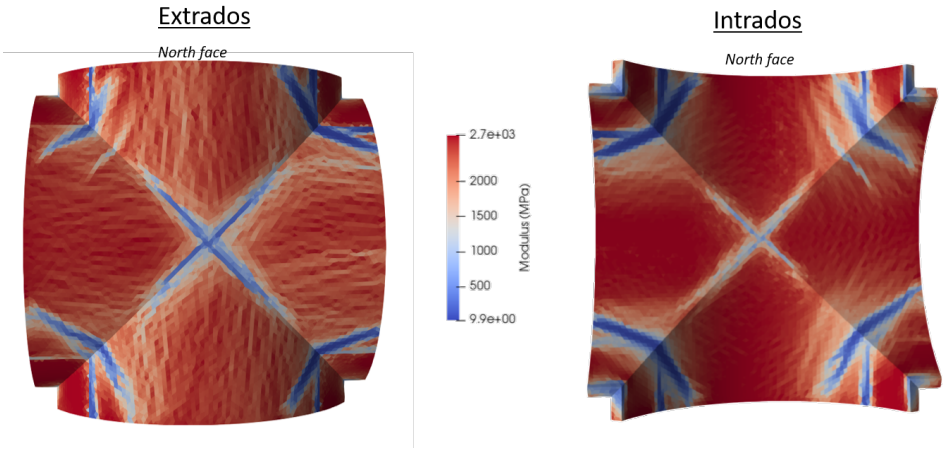

Figure 11. Field of damaged modulus used for the modal calculus.

Anyway some limitations may be highlighted :

- *Geometrical model generation.* On one side the CHM needs a volumic mesh of the overall structure and on the other side the BBM needs a volumic mesh of each block of the structure. Clearly the block by block approach may needs a huge amount of work to address real life structures, even if it exists algorithm able to subdivide automatically 3D volumes (inspired from Bagneris et al. (2010)). The cost of geometrical modeling with respect to the computation was discussed by Ferrante (Ferrante (2021c)).
- *Intrinsic limitations of the models.* On one side the CHM, depending on the complexity of the described phenomenology, may need an important number of parameters and its non linear response is essentially driven by the mechanical loads and not by the stereotomy. Characterization of all the parameters is complicated since they concern the equivalent masonry material. As illustrated on figure 6 our CHM model was able to catch the main diagonal fractures but these fractures were not kicking to follow the joints. Furthermore, for such approaches it is more complicated to compute the progressive collapse of the structure, lets say the large motion of groups of block. On the other side the BBM needs less mechanical parameters, even if they might be complicated to determine. In such approach the overall non linear behavior is essentially driven by the behavior of the joints and cannot take into account the fracture of the blocks without subdividing them, adding a priori potential crack path. Finally this approach is capable to compute the partial or total collapse of the structure.
- *Computational time.* The CHM is clearly more efficient. Concerning the seismic example, CHM took around 14 days of sequential time when BBM took around 29 days of sequential time. Furthermore taking advantage of parallel computing is easier with CHM than BBM, since some parts of the multi-contact solver are inherently sequential.

Future development work aims at optimizing an hybrid FEM-DEM approach, incorporating thermal damage considerations, and applying the methodology to damaged masonry vaults, such as those in the Notre-Dame de Paris cathedral, within the French research grant DEMMEFI project. These endeavors mark crucial targets for advancing the capabilities and applications of the proposed hybrid FEM-DEM method. Other issues to be considered in the future include the study of strengthened masonry structures and the improvement of guidelines for the use of the novel hybrid approach. All of these aspects are already underway.

Acknowledgement

This work was carried out within the framework of the DEMMEFI research project (ANR-20-CE22-0004) supported by the French National Research Agency (ANR). The authors are grateful to the ANR for its financial support.

References

Bagneris, M., Marty, A., Maurin, B., Motro, R., Pauli, N. 2010. Pascalian forms as morphogenetic tool. *Journal of the International Association for Shells and Spatial Structures*, 51, pp. 165-181.

Bianchini, N. and Calderini, C. and Mendes, N. and Candeias, P. and Lourenço, P.B. 2023. Blind Prediction Competition - Sera.ta - Seismic Response of Masonry Cross Vaults: Shaking table tests and numerical validations (Version 1) [Data set]. *Zenodo. https://doi.org/10.5281/zenodo.7624666.*

Bianchini, N. and Calderini, C. and Mendes, N. and Candeias, P. and Lourenço, P.B. 2023. Postdiction Competition - Sera.ta - Seismic Response of Masonry Cross Vaults: Shaking table tests and numerical validations (Version 1) [Data set]. *Zenodo. https://doi.org/10.5281/zenodo.7624791.*

Boukham, A. and Parent, T. and Morel, S. and Dubois, F. and Mindeguia, J.C. 2023. Discrete element modelling of a masonry wall subjected to shear with taking into account the damage of blocks. *AJCE*, 41.

D'Altri, A.M., Sarhosis, V., Milani, G., Rots, J., Cattari, S., Lagomarsino, S., Sacco, E., Tralli, A., Castellazzi, G., De Miranda, S. 2019. Modeling Strategies for the computational analysis of unreinforced masonry structures: Review and classification. *Arch. Comp. Meth. Eng.*

D'Ayala, D.F. and Tomasoni, E. 2011. "Three-Dimensional Analysis of Masonry Vaults Using Limit State Analysis with Finite Friction". *Int. J. Archit. Herit.* 5, 140–171.

Domede, N. and Sellier, A. and Stablon, T. 2013. Structural analysis of a multi-span railway masonry bridge combining in situ observations, laboratory tests and damage modelling. *Engineering Structures*, 56, 837-849.

Drucker, D.C. and Prager, W. 1952. Soil mechanics and plastic analysis or limit design. *Q. Appl. Math.* 10, 157–165.

Dubois, F. and Jean, M. 2006. The non smooth contact dynamic method: recent LMGC90 software developments and application. *Wriggers, P., Nackenhorst, U. (eds) Analysis and Simulation of Contact Problems. Lecture Notes in Applied and Computational Mechanics, vol 27. Springer, Berlin, Heidelberg.* https://doi.org/10.1007/3-540-31761-9_44

Dubois, F. and Acary, V. and Jean, M. 2018. The Contact Dynamics method: A nonsmooth story. *Comptes Rendus Mécanique* 346, 247–262. https://doi.org/10.1016/j.crme.2017.12.009

Ferrante, A. and Loverdos, D. and Clementi, F. and Milani, G. and Formisano, A. and Lenci, S. and Sarhosis, V. 2021. Discontinuous approaches for nonlinear dynamic analyses of an ancient masonry tower. *Eng. Struct.* 230, 111626. https://doi.org/10.1016/j.engstruct.2020.111626

Ferrante, A. and Schiavoni, M. and Bianconi, F. and Milani, G. and Clementi, F. 2021. Influence of Stereotomy on Discrete Approaches Applied to an Ancient Church in Muccia, Italy. *J. Eng. Mech.* 147.

Ferrante, A. 2021. Computational strategies for discrete modeling of Cultural Heritage structures. *PhD, Polytechnic University of Marche*

Gaetani, A. and Monti, G. and Lourenço, P.B. and Marcari, G. 2016. Design and Analysis of Cross Vaults Along History. *Int. J. Archit. Herit.* 10, 841–856.

Hillerborg, A. and Modéer, M. and Petersson, P.-E. 1976. Analysis of crack formation and crack growth in concrete by means of fracture mechanics and finite elements. *Cem. Concr. Res.* 6, 773–781.

Jean, M. 1999. The non-smooth contact dynamics method. *Comput. Methods Appl. Mech. Eng.* 177, 235–257.

Lourenço, P.B. and Rots, J.G. 1997. Multisurface Interface Model for Analysis of Masonry Structures. *J. Eng. Mech.* 123, 660–668.

Moreau, J.J. 1988. Unilateral Contact and Dry Friction in Finite Freedom Dynamics, in: *Nonsmooth Mechanics and Applications.* Springer Vienna, Vienna, pp. 1–82.

Parent, T. and Brocato, M. and Colas, A.S. and Domede, N. and Dubois, F. and Garnier, D.

and Gros, A. and Mindeguia, J.-C. and Morel, S. and Morenon, P. and Nougayrede, P. and Taforel, P. 2023. A multi-model structural analysis of the vaults of Notre-Dame de Paris Cathedral after the 2019 fire and a proposal for a hybrid model merging continuum and discrete approaches. in: *Journal of Cultural Heritage*.

Roca, P., Cervera, M., Gariup, G., Pela, L. 2010. Structural analysis of masonry historical construction. Classical and advanced approaches. *Arch. Comp. Meth. Eng.*.

Rossi, M. and Calderini, C. and Lagomarsino, S. 2016. Experimental testing of the seismic in-plane displacement capacity of masonry cross vaults through a scale model. *Bull. Earthq. Eng.* 14, 261–281.

Sellier, A. and Casaux-Ginestet, G. and Buffo-Lacarrière, L. and Bourbon, X. 2013. Orthotropic damage coupled with localized crack reclosure processing. Part I: Constitutive laws. *Eng. Fract. Mech.* 97, 148–167.

Sellier, A. and Morenon, P. and Domède, N. 2022. Computational performances optimization of a mechanical behaviour model for geomaterials, in: *RUGC* 40 (1), 207–210. doi:10.26168/ajce.40.1.51.

SERA project (2021). SERA project reference 730900 - SERA, call H2020-INFRAIA-2016-1. URL https://sera-crossvault.wixsite.com/blindprediction

Venzal, V. and Morel, S. and Parent, T. and Dubois F. 2020. Frictional cohesive zone model for quasi-brittle fracture: Mixed-mode and coupling between cohesive and frictional behaviors. *Int. J. Solids Struct.* 198, 17–30.